

## Supporting Information

### **Poly(Vinylidene Fluoride)-Passivated CsPbBr<sub>3</sub> Perovskite Quantum Dots with Near-Unity Photoluminescence Quantum Yield and Superior Stability**

Lin Yang,\* Bowen Fu, Xu Li, Hao Chen, and Lili Li,

*College of Physics Science and Technology, Hebei University, Baoding 071002, Hebei, P. R. China*

*\* Corresponding authors. Tel.: +86 312 5077069; fax: +86 312 5077069.*

*E-mail addresses: yanglin@hbu.edu.cn (L.Yang).*

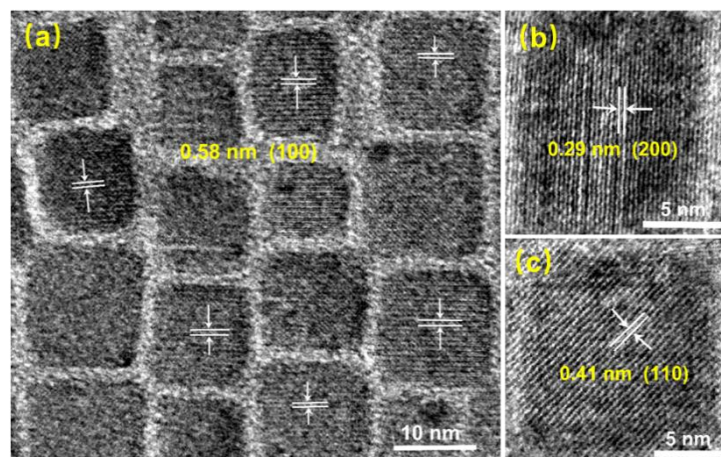


**Figure S1.** HRTEM of PVDF-CsPbBr<sub>3</sub> QDs reflecting the crystal planes of (100), (200), and (110), respectively.

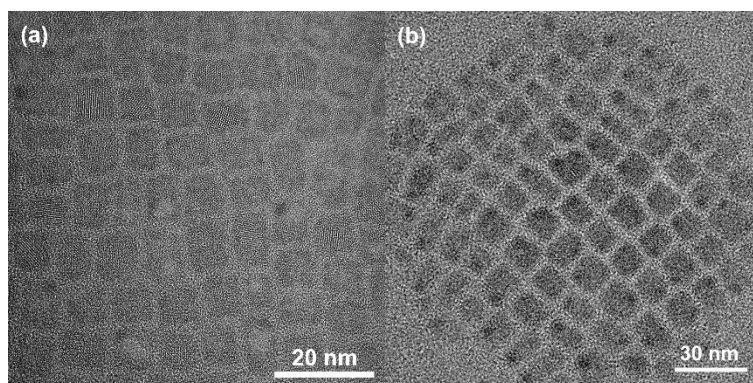


**Figure S2.** TEM images of the (a) pristine CsPbBr<sub>3</sub> and (b) PVDF-CsPbBr<sub>3</sub> QDs after exposure in ambient condition for 60 days

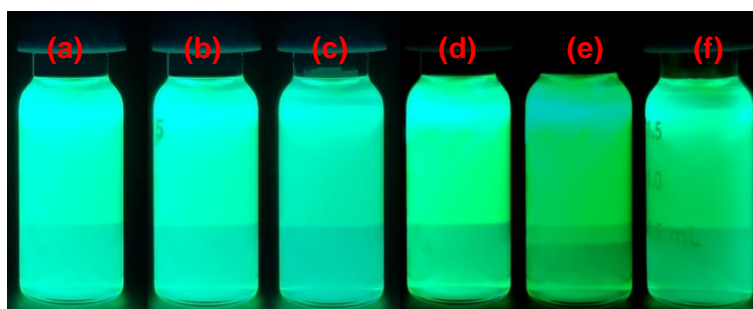


**Figure S3.** Photographs of the pristine CsPbBr<sub>3</sub> QDs samples taken under a UV lamp after exposure in ambient condition for (a) 0, (b) 3, (c) 7, (d) 15, (e) 30, and (f) 60 days, respectively.

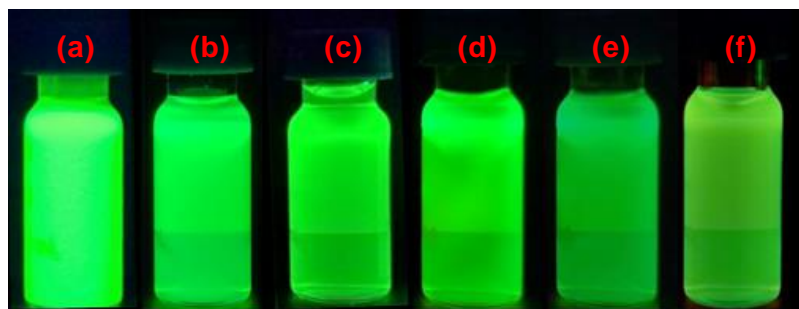


**Figure S4.** Photographs of the PVDF-CsPbBr<sub>3</sub> QDs samples taken under a UV lamp after exposure in ambient condition for (a) 0, (b) 3, (c) 7, (d) 15, (e) 30, and (f) 60 days, respectively.

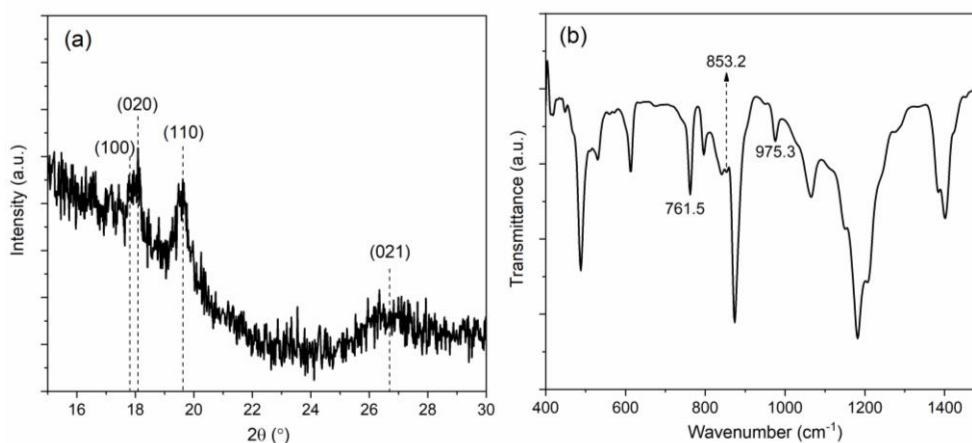


**Figure S5.** XRD pattern and FTIR spectrum of the raw PVDF used in our study.

The raw PVDF exhibit characteristic diffraction pattern for the  $\alpha$ -phase, as shown in Figure S4. It presents three prominent diffraction peaks at 17.8°, 18.1° and 19.6°, which are relative to the (100), (020) and (110) planes of  $\alpha$ -phase, respectively. Additionally, the XRD pattern also shows a diffraction peak of (021) plane at 26.7°, allowing a clear identification of  $\alpha$ -phase PVDF. In addition, the phase of PVDF is most easily detected by FTIR, as it presents a large number of characteristic bands, such as the absorption bands at 761.5 cm<sup>-1</sup> (CF<sub>2</sub> bending), 853.2 cm<sup>-1</sup> (C-C skeletal bending) and 975.3 cm<sup>-1</sup> (CH out-of-plane deformation), which is unavailable for  $\beta$  and  $\gamma$ -phases.

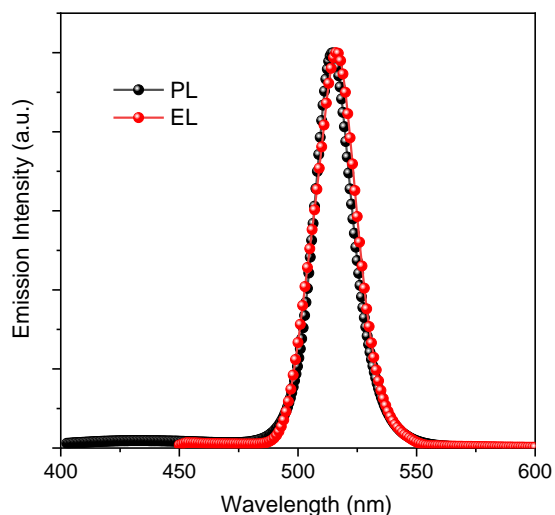


**Figure S6.** PL spectrum of PVDF-CsPbBr<sub>3</sub> film and EL spectrum of PVDF-CsPbBr<sub>3</sub> QLED.

**Table S1.** Fitting parameters of the time-resolved PL decay, PLQY,  $K_{et}$  and  $K_{net}$  values of pristine CsPbBr<sub>3</sub> and PVDF-CsPbBr<sub>3</sub> QDs.

	$A_1$ (%)	$\tau_1$ (ns)	$A_2$ (%)	$\tau_2$ (ns)	$A_3$ (%)	$\tau_3$ (ns)	$\tau_{ave}$ (ns)	PLQY (%)	$K_{et} \times 10^7$ (s <sup>-1</sup> )	$K_{net} \times 10^7$ (s <sup>-1</sup> )
Pristine CsPbBr <sub>3</sub>	22.24	0.79	51.97	1.32	25.79	6.28	2.48	82	33.06	7.26
PVDF-CsPbBr <sub>3</sub>	15.15	1.68	84.85	12.32	–	–	10.71	98	9.15	0.19

**Table S2.** Performance parameters of QLED devices: EL (electroluminescence),  $V_{on}$  (turn-on voltage), L (Luminance), EQE (external quantum efficiency), CE (current efficiency), and PE (power efficiency).

QDs	EL $\lambda_{max}$ (nm)	$V_{on}$ (V)	Max. L (cd m <sup>-2</sup> )	Max. EQE (%)	Max. CE (cd A <sup>-1</sup> )	Max. PE (lm W <sup>-1</sup> )
Pristine CsPbBr <sub>3</sub>	517	3.88	5055	0.84	1.84	1.80
PVDF-CsPbBr <sub>3</sub>	516	3.93	5711	1.71	4.25	3.90